DOI: 10.1002/chem.201103761

An Optimised Small-Molecule Stabiliser of the 14-3-3–PMA2 Protein–Protein Interaction

Anja Richter,[b] Rolf Rose,[a] Christian Hedberg,[b] Herbert Waldmann,*[b, c] and Christian Ottmann*[a]

Abstract: Modulation of protein–protein interactions (PPIs) is a highly demanding, but also a very promising approach in chemical biology and targeted drug discovery. In contrast to inhibiting PPIs with small, chemically tractable molecules, stabilisation of these interactions can only be achieved with complex natural products, like rapamycin, FK506, taxol, forskolin, brefeldin and fusicoccin. Fusicoccin stabilises the activatory complex of the plant H^+-ATPase PMA2 and 14-3-3 proteins. Recently, we have shown that the stabilising effect of fusicoccin could be mimicked by a trisubstituted pyrrolinone (pyrrolidone1, **1**). Here, we report the synthesis, functional activity and crystal structure of derivatives of **1** that stabilise the 14-3-3–PMA2 complex. With a limited compound collection three modifications that are important for activity enhancement could be determined: 1) conversion of the pyrrolinone scaffold into a pyrazole, 2) introduction of a tetrazole moiety to the phenyl ring that contacts PMA2, and 3) addition of a bromine to the phenyl ring that exclusively contacts the 14-3-3 protein. The crystal structure of a pyrazole derivative of **1** in complex with 14-3-3 and PMA2 revealed that the more rigid core of this molecule positions the stabiliser deeper into the rim of the interface, enlarging especially the contact surface to PMA2. Combination of the aforementioned features gave rise to a molecule (**37**) that displays a threefold increase in stabilising the 14-3-3–PMA2 complex over **1**. Compound **37** and the other active derivatives show no effect on two other important 14-3-3 protein–protein interactions, that is, with CRaf and p53. This is the first study that describes the successful optimisation of a PPI stabiliser identified by screening.

Keywords: chemical synthesis · crystal structures · protein–protein interactions · structure–activity relationships · X-ray crystallography

Introduction

Targeted drug discovery mainly concentrates on the development of enzyme active site inhibitors. Although the highly promising field of protein–protein interaction (PPI) modulation has been elaborated with molecules that disrupt PPIs,[1] the reverse strategy to stabilise PPIs with small, drug-like molecules is underrepresented in medicinal chemistry research.

An interesting case of PPIs is typified by the 14-3-3 protein family. These highly conserved, small (25–30 kDa) eukaryotic adapter proteins influence a plethora of physiological processes by binding to hundreds of diverse protein partners.[2,3] They bind their targets through short phosphorylated sequences and modulate their partners' subcellular localisation, enzymatic activity or their ability to interact with further proteins.[3–5] The seven human isoforms (β, γ, ε, η, σ, τ, and ζ) regulate the activity of, for example, the kinase CRaf,[6,7] the cell-cycle phosphatase Cdc25,[8,9] the transcriptional modulator YAP,[10,11] and stabilise the tumour suppressor p53.[12,13] The 14-3-3 proteins have been implicated in a variety of human diseases. In addition to their participation in diverse cancers,[14] they have been associated with the development of neurodegenerative diseases[15] or virulence of human pathogenic organisms.[16,17]

The natural product fusicoccin A (FC-A)[18] produced by the phytopathogenic fungus *Phomopsis amygdali* is a natural modulator of a 14-3-3 protein–protein interaction and targets the complex of the plant plasma membrane H^+-ATPase (PMA) and 14-3-3 proteins.[19] FC-A binds to the interface of the activated complex and enhances the affinity of the two protein partners approximately 90-fold.[20] This stabilisation induces permanent activation of the proton pump, which translates into the maximal opening of the plants' gas-exchanging stomatal pores and subsequent wilting.[21] Hence, FC-A is a potent herbicidal compound, but its complex chemical structure and the potentially high costs of

[a] Dr. R. Rose,[+] Dr. C. Ottmann
Chemical Genomics Centre of the Max-Planck-Society
Otto-Hahn-Strasse 15, 44227 Dortmund (Germany)
E-mail: christian.ottmann@cgc.mpg.de

[b] Dr. A. Richter,[+] Dr. C. Hedberg, Prof. Dr. H. Waldmann
Department of Chemical Biology
Max Planck Institute of Molecular Physiology
Otto-Hahn-Strasse 11, 44227 Dortmund (Germany)
E-mail: herbert.waldmann@mpi-dortmund.mpg.de

[c] Prof. Dr. H. Waldmann
Fakultät Chemie, Fachbereich Chemische Biologie
Technische Universität Dortmund
Otto-Hahn-Strasse 6, 44227 Dortmund (Germany)

[+] These authors contributed equally to this work.

Supporting information for this article is available on the WWW under http://dx.doi.org/10.1002/chem.201103761.

production most likely would prevent a successful practical application. Therefore, by screening a compound library we set out to identify synthetically more accessible molecules that show stabilising activity towards 14-3-3–PMA.

As a result we recently reported that epibestatins and pyrrolinones stabilise the PMA (isoform 2)–14-3-3 interaction.[22] The crystal structures of the corresponding ternary complexes could be solved and explained the different dynamics of their mode of action. These molecules bind to the rim of the interface of 14-3-3 and PMA2 establishing contacts to both protein partners and show promising physiological activity in a stomata-opening assay. Consequently, they might be good starting points for the development of novel herbicides with an as yet not explored mode of action.

Here, we report the synthesis of a pyrrolinone collection starting from the initial screening hit **1**.[22] We determined

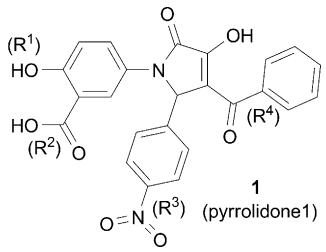

1 (pyrrolidone1)

their binding mode by solving the crystal structure of one compound of this collection in complex with 14-3-3 and the last C-terminal 30 amino acids of PMA2 harbouring a phosphothreonine-mimicking aspartate as penultimate residue (PMA2-CT30YDI). One pyrazole analogue of the guiding heterocycle showed enhanced stabilising activity towards the 14-3-3–PMA2 complex and is selective for this 14-3-3 PPI.

Results and Discussion

Synthesis of derivatives of 1: In order to identify possible chemical derivatisations that enhance the stabilising activity of the initial hit **1** a small focused compound library of pyrrolinones and pyrazoles with different substitution patterns was prepared (Tables 1 and 2). In detail, the hydroxyl group at R^1 was either preserved (**1**, **2**, **5**, **9**, **13**, **17**, **27**, **32**, **33**, **35**), changed to a carboxyl (**4**, **7**, **11**, **14**, **19**, **22**, **29**, **31**, **34**, **36**) or omitted (**3**, **6**, **8**, **10**, **12**, **15**, **16**, **18**, **20**, **21**, **23**–**26**, **28**, **30**, **37**). The carboxyl group at R^2 was kept in 18 out of 37 derivatives. In **8**, **16**, **20**, **23**, **24**, **26**, **30**, and **37** it was replaced by a tetrazole moiety, and in **4**, **7**, **11**, **12**, **14**, **19**, **22**, **29**, **31**, **34**, and **36** it was changed to a proton. For R^3 the nitro group was replaced by carboxylic acid (**2**–**4**, **9**–**12**, and **17**–**20**), thiazole (**13**, **14**, **21**–**23**, **25**–**30**, and **35**) or bromine (**33**). At R^4 either a methoxy substituent (**5**–**14**, **25**, **26**, and **36**) or bromine (**15**–**20**, **27**–**30**, and **37**) was introduced. Conversion of the corresponding pyrrolinone into a pyrazole rigidifies the molecule, potentially enhancing binding affinity by reducing the entropy penalty upon binding to the protein complex.

Table 1. Derivatives of 1 prepared by Doebner condensation.

Cmp[a]	R^1	R^2	R^3	R^4	Yield[b] [%]
1	OH	COOH	NO_2	H	
2	OH	COOH	COOH	H	6
3	H	COOH	COOH	H	11
4	COOH	H	COOH	H	9
5	OH	COOH	NO_2	OMe	12
6	H	COOH	NO_2	OMe	56
7	COOH	H	NO_2	OMe	33
8	H	tetrazo-5-yl	NO_2	OMe	9
9	OH	COOH	COOH	OMe	26
10	H	COOH	COOH	OMe	25
11	COOH	H	COOH	OMe	30
12	H	H	COOH	OMe	25
13	OH	COOH	thiazo-2-yl	OMe	18
14	COOH	H	thiazo-2-yl	OMe	32
15	H	COOH	NO_2	Br	64
16	H	tetrazo-5-yl	NO_2	Br	58
17	OH	COOH	COOH	Br	42
18	H	COOH	COOH	Br	38
19	COOH	H	COOH	Br	27
20	H	tetrazo-5-yl	COOH	Br	23
21	H	COOH	thiazo-2-yl	H	21
22	COOH	H	thiazo-2-yl	H	7
23	H	tetrazo-5-yl	thiazo-2-yl	H	16
24	H	tetrazo-5-yl	NO_2	H	5
25	H	COOH	thiazo-2-yl	OMe	45
26	H	tetrazo-5-yl	thiazo-2-yl	OMe	29
27	OH	COOH	thiazo-2-yl	Br	34
28	H	COOH	thiazo-2-yl	Br	19
29	COOH	H	thiazo-2-yl	Br	33
30	H	tetrazo-5-yl	thiazo-2-yl	Br	32
31	COOH	H	NO_2	H	20

[a] All compounds were at least 80% pure; [b] chemical synthesis yield.

Table 2. Pyrazole derivatives of **1**.

Cmp[a]	R^1	R^2	R^3	R^4	Yield[b] [%]
32	OH	COOH	NO_2	H	72
33	OH	COOH	Br	H	75
34	COOH	H	NO_2	H	77
35	OH	COOH	thiazo-2-yl	H	78
36	COOH	H	NO_2	OMe	77
37	H	tetrazo-5-yl	NO_2	Br	71

[a] All compounds were at least 80% pure; [b] chemical synthesis yield.

Initially all pyrrolinones listed in Table 1 and all pyrazoles listed in Table 2 entries 1–5 were prepared.

Derivatives of 1 stabilise the 14-3-3–PMA2 interaction: To investigate the stabilising activity of the synthesised compound collection we employed a surface-based assay. In brief, the binding of green fluorescent protein (GFP)-tagged 14-3-3 to surface-immobilised PMA2-CT66 (the C-terminal 66 amino acids of PMA2) fused with gluthatione *S*-transferase (GST) was monitored in the presence of the candidate compounds. To compare the stabilising activity of the tested compounds all fluorescence values were normalised to the activity of **1**, which was set to 100% (Figure 1).

Of the alterations described above (Tables 1 and 2), all were detrimental in terms of stabilising activity with the exception of the pyrazole derivative (**32**) of **1** (Figure 1).

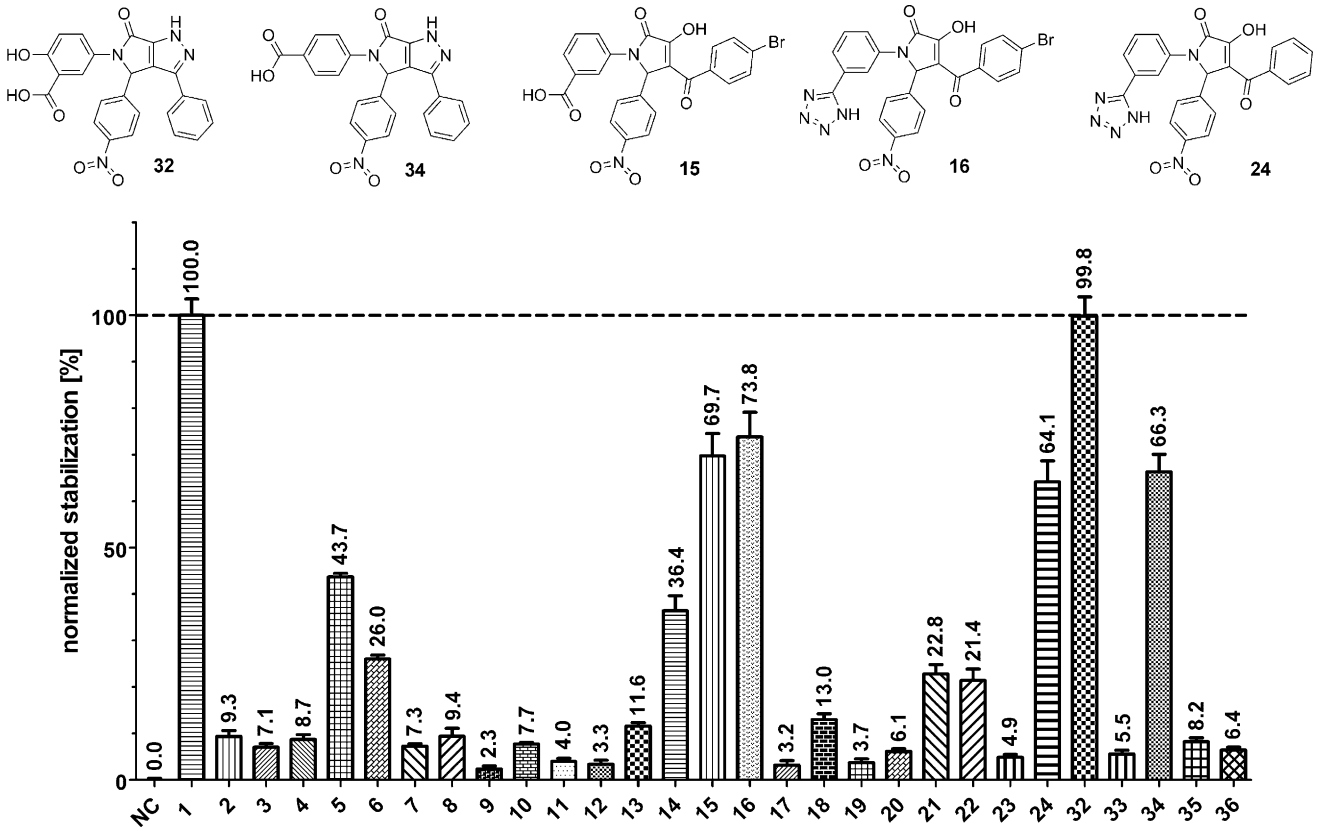

Figure 1. Compounds stabilising the PMA2–14-3-3 interaction. Structures and activities of compounds from the library of derivatives of **1**. The stabilising activities of the candidate molecules were normalised to the HTS-Hit **1**. Binding of the GFP-fused tobacco 14-3-3 protein T14-3e to immobilised PMA2-CT66YDI in the presence of the compounds was measured by using a surface-based assay (see the Experimental Section). NC: no compound control.

Nonetheless, compounds **34**, **15**, **16**, and **24** showed normalised activities above 50% of **1**. Notably, of these, compound **34**, like **32**, is also a pyrazole. The other derivatives that still showed activity were characterised by either a bromine at R^4 (**15** and **16**) or/and a tetrazole moiety at R^2 (**16** and **24**). Of these compounds EC_{50} values were determined (Figure 2). As expected from the single concentration measurements these values were quite similar, ranging from 286-(±62) μM (**16**), over 307(±81) μM (**15**) and 368(±96) μM (**24**) to 383(±82) μM (**34**). In order to elucidate the mechanistic basis of the influence of the chemical modifications on the protein complex, we pursued the co-crystallisation of the compounds with 14-3-3e and PMA2-CT30YDI and succeeded in the case of **34**.

Structure of 34 in complex with T14-3e–CT30YDI: Crystals of **34** in complex with the tobacco 14-3-3 protein T14-3e and the PMA2 C-terminal construct CT30YDI appeared after 5–7 days in CHES (0.1 M, pH 9.5), LiCl (1.0 M) and sucrose (30% w/v) at 4°C and grew to dimensions of 500×500×300 μm within two weeks. They diffracted to 3.4 Å and the electron density allowed building of 225 out of 231 residues of T14-3e and the complete 30 residues of CT30. Details of the statistics of the crystal structure are summarised in Table 3.

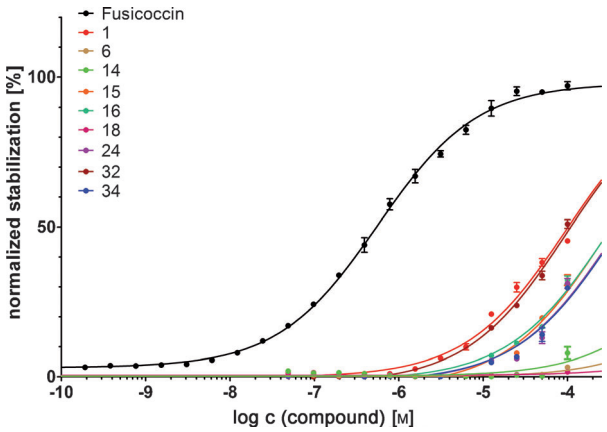

Figure 2. Activity of PMA2–14-3-3 stabilising compounds compared to **1**. Binding of GFP–T14-3c to immobilised GST–CT52YDI in response to the concentration of the stabilising molecules. For comparison the binding curve for fusicoccin is shown in black.

Despite the rather low resolution, the solvent flattened electron density for **34** was good (Figure 3a, b) and allowed the determination of the binding of **34** to the complex of T14-3e and PMA2-CT30YDI (Figure 3c, d, f). The 14-3-3 protein displayed the typical dimeric form with one PMA2-

Table 3. Crystallographic data.[a] (PDB ID: 4DX0)

cell dimensions [Å]	98.450, 98.450, 216.710
space group	I4122
resolution [Å]	3.4 (3.6–3.4)
observations	45606 (7284)
unique Reflections	7386 (1131)
completeness [%]	96.1 (97.6)
I/σ	13.98 (3.77)
R_{sym} [%]	10.3 (43.0)
R_{cryst} [%]	32.4
R_{free} [%]	36.2
protein atoms	2020
ligand atoms	33
R.m.s.d. of bond length, count; RMS; weight [Å]	2073; 0.007; 0.022
R.m.s.d. of isotropic thermal factor, count; RMS; weight [Å^2]	1248; 0.370; 1.500
m.c. bond	2001; 0.676; 2.000
m.c. angle	825; 0.436; 3.000
s.c. bond	794; 0.791; 4.500
s.c. angle	

[a] Data for the outermost shell are shown in parentheses.

CT30YDI peptide bound to each of the monomers (Figure 3c).

The pyrazole **34** occupies a pocket that is concomitantly formed by both proteins (Figure 3d, f) and largely matches that of **1** (Figure 3e). As with **1** most of the contact surface is contributed by the 14-3-3 protein; this might explain the rather weak activity of both compounds with respect to stabilising the T14-3e–PMA2-CT30YDI complex. Nevertheless, in comparison with **1**, **34** is localised nearer to a narrow cleft between T14-3e and PMA2-CT30YDI (Figure 3f). This positions the molecule deeper into the rim of the protein–protein interface, which is desirable for a PPI stabilising compound. The fact that **34** is weaker than **1** in stabilising the 14-3-3–PMA2 complex might be due to the carboxylate at R^1 and a missing substituent at R^2. Compound **32**, for example, stabilises the complex more strongly and bears a hydroxyl group at R^1 and a carboxylate at R^2.

Derivatives with enhanced stabilising potency: The structural analysis of **34** in complex with T14-3e–PMA2-CT30YDI prompted us to elongate **34** in R^1 to fill the remaining space

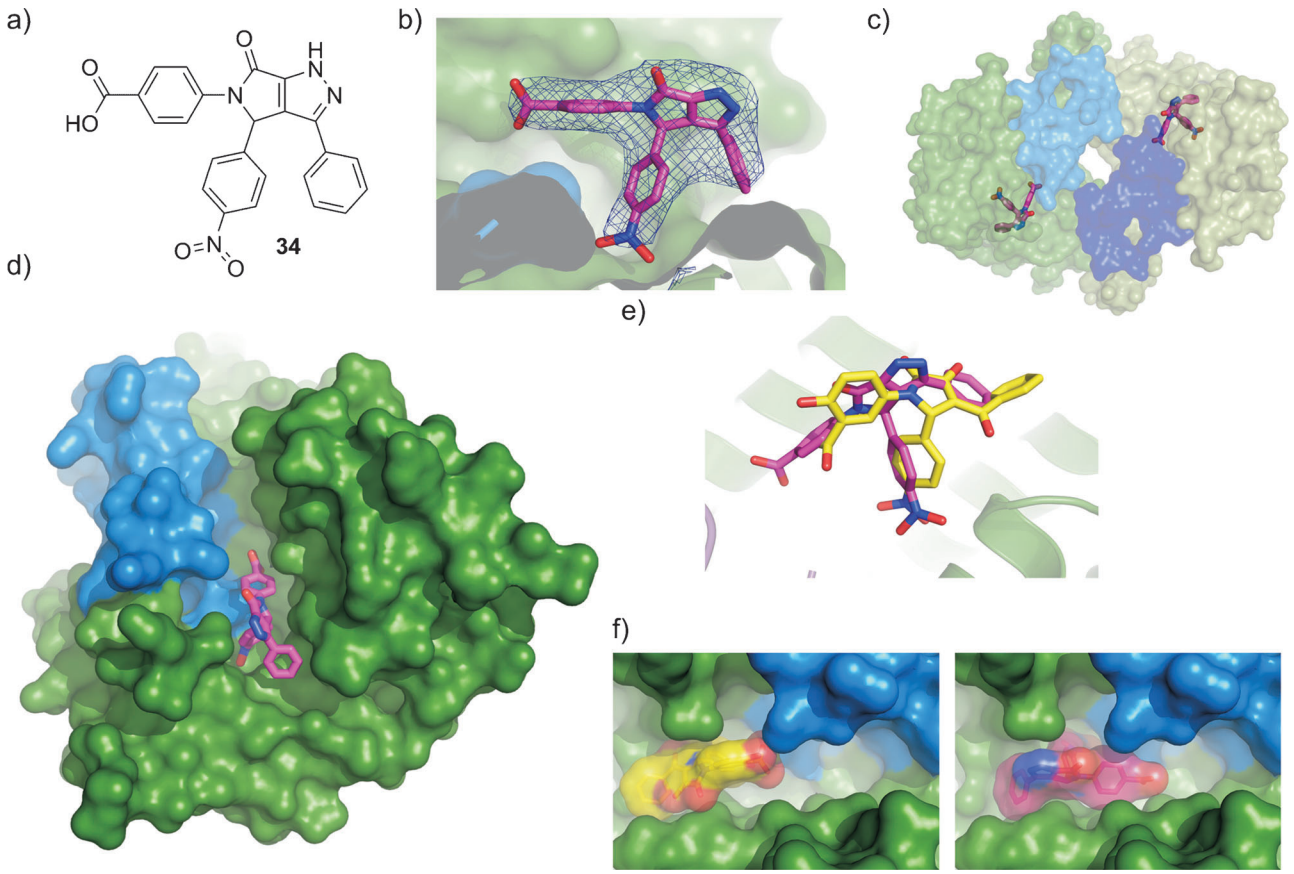

Figure 3. Crystal structure of **34** in complex with T14-3e and PMA2-CT30YDI (PDB ID: 4DX0). a) Structure of **34**. b) Final $2F_o$-F_c electron density (blue mesh, contoured at 1σ) of **34** (magenta sticks) binding to the interface of T14-3e (green, semitransparent surface) and PMA2-CT30YDI (blue, semitransparent surface). c) Overview of the T14-3e dimer (dark and light-green, semitransparent surface) complexed with PMA2-CT30YDI (dark and light-blue, semitransparent surface) and **34** (magenta sticks). d) Binding of **34** (magenta sticks) to a T14-3e monomer (green surface) complexed with PMA2-CT30YDI (blue surface). e) Superimposition of **1** (yellow sticks, PDB ID: 3M51) and **34** (magenta sticks) bound to the T14-3e–PMA2-CT30YDI complex. f) Binding of **1** (yellow sticks and semitransparent surface) and **34** (magenta sticks and semitransparent surface) to the rim of the interface of T14-3e (green surface) and PMA2-CT30YDI (blue surface). NC: no compound control.

in the interface of the two proteins (Figure 3 f). This was attempted by the generation of amides (Table S1 in the Supporting Information). The resulting molecules derived from **34** were expected to form additional interactions with the PMA2-CT30YDI surface (Figure 3 f, blue surface). However, none of these amides showed any stabilising effect on the 14-3-3–PMA2 complex in the surface-based assay (data not shown). In a second approach we combined all chemical modifications represented in the initial library that were compatible with stabilising the 14-3-3–PMA2 interaction. These are: 1) conversion into a pyrazole, 2) a tetrazole moiety at R^2, and 3) a bromine at R^4. This combination gave rise to molecule **37** (Table 2, entry 6, Figure 4).

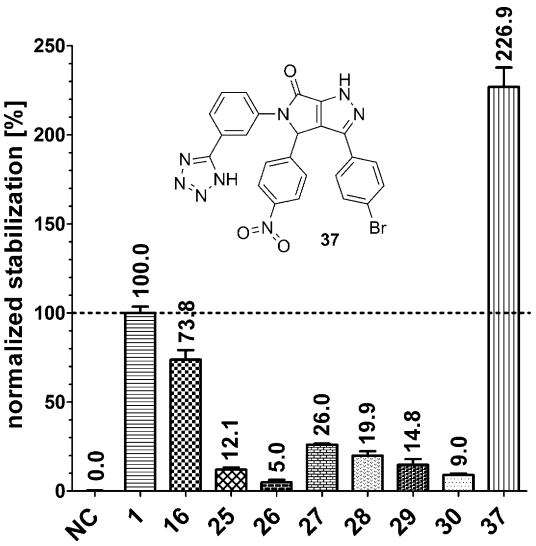

Figure 4. The optimised compound **37** stabilises the PMA2–14-3-3 interaction more strongly than **1**. The stabilising activities of the candidate molecules were normalised to the HTS-Hit **1**. Binding of the tobacco, GFP-fused 14-3-3 protein, T14-3e, to immobilised PMA2-CT52YDI in the presence of the compounds was measured by using a surface-based assay (see the Experimental Section).

Compound **37** was tested in the surface-based assay at a single concentration (100 μM) and was found to be significantly more active than **1** (Figure 4 and Figure 5). Here, especially interesting is the fact that the pyrazole **37** was about three-times more active than its pyrrolinone counterpart **16**; this supports the pyrazole scaffold as being more suited than the pyrrolinone. Another way to compare the compound's stabilising activity towards the 14-3-3–PMA2 complex is the determination of the EC_{50} (Figure 5). Here, formation and endurance of the GST–PMA2-CT66–GFP–T14-3c complex is monitored at different concentrations of compounds. As a reference we determined the EC_{50} of the natural product FC-A to 498(±65) nM (Figure 5). Compound **1** displays a stabilising activity of 101(±13) μM and **37** showed an EC_{50} of 33(±4) μM.

A structural explanation for the enhanced activity of 37 over 1 and 34: Comparison of the crystal structures of **1** (Figure 6 a) and **34** (Figure 6 b) bound to the T14-3e–CT30YDI complex allowed some explanation of the results from the surface-based stabilisation assay with the compounds from the first round of synthesis (Figure 1) and provided a possible rationale for the enhanced activity of **37** (modelled in Figure 6 c). One crucial point in enhancing the stabilisation the 14-3-3–CT30YDI complex by derivatives of **1** is to strengthen the binding of the small molecule to CT30YDI. The extreme C-terminal Ile956 of CT30YDI plays a special role in this context. In the T14-3c–CT52–FC-A complex the side chain and the free C terminus of this residue make the main contacts between CT52YDI and FC-A.[23] Furthermore, the crystal structure of **34** bound to the T14-3e–CT30YDI binary complex (this study) revealed a relatively large pocket near Ile956 conjointly formed by both protein partners. Modelling of **37** into the binding pocket of **34** in the experimentally solved structure suggests that the tetrazole moiety at R^2 could at least partially fill this pocket; this would establish simultaneous contacts to Ile956 of CT30YDI as well as Ser52, Ile175 and Ile226 of T14-3e (Figure 6 c). Since compounds **15** and **16** showed that bromine at R^4 was compatible with stabilisation of the complex (Figure 1) we introduced this substitution into **37** (Figure 4). As the modelling suggests, the hydrophobic contact surface to Phe126 of T14-3e should be increased by this modification (Figure 6 c) most probably accountings for a positive overall effect on the stabilising activity.

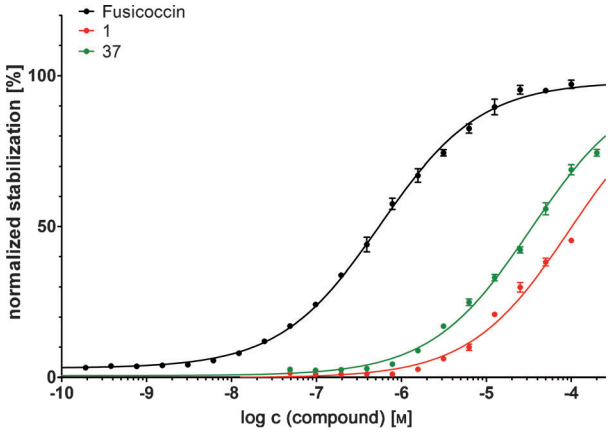

Figure 5. Enhanced stabilising activity of **37** compared to **1**. Binding of GFP–T14-3c to immobilised GST–CT52YDI in response to the concentration of the stabilising molecules. For comparison the binding curve for fusicoccin is shown in black.

Specificity of derivatives of 1 for the 14-3-3–PMA2 complex stabilisation: Since 14-3-3 proteins interact with hundreds of proteins in eukaryotic organisms,[3] specificity of pharmacological intervention is an important issue. We employed our surface-based assay to test a potential stabilising effect of derivatives of **1** towards the 14-3-3 PPI with CRaf and p53. Protein 14-3-3 binds to CRaf through the phosphorylation sites pS233, pS259 and pS621.[6] Protein p53 is bound to 14-3-3 through its C-terminal phosphorylation sites pS378 and

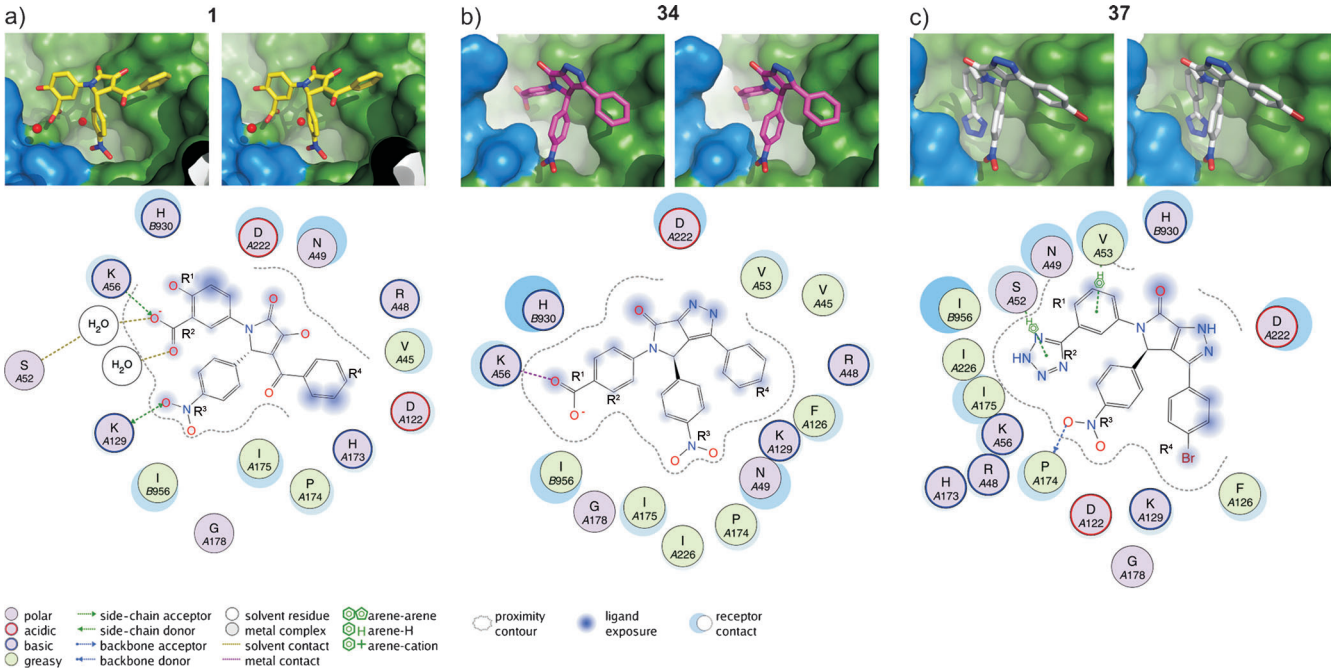

Figure 6. Details of the binding modes of **1** and derived molecules. Upper row: stereo figures of the compounds in their protein target pockets. Lower row: schemes of the binding mode produced with MOE (http://www.chemcomp.com/). a) Compound **1** bound to T14-3e–CT30YDI (PDB ÍDID: 3M51). b) Compound **34** bound to T14-3c–CT30YDI (this study). c) Compound **37** modelled into the **34** binding pocket.

pT387.[12] As shown in Figure 7, all six compounds display a stabilising effect towards binding of 14-3-3 proteins to GST–PMA2-CT52YDI without showing any interference with GST–$p53_{319–393}$ or GST–$CRaf_{229–268}$.

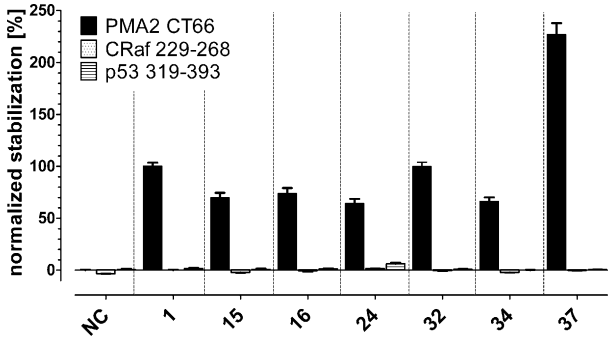

Figure 7. Specificity of **37** and other derivatives of **1** to the PMA2–14-3-3 protein–protein interaction. The specificity of compounds from this study was tested by measuring their stabilising potential towards the 14-3-3 protein–protein interaction with the 14-3-3 binding motif from CRaf and p53, both of which were fused to GST.

The versatile and widespread biological functions of 14-3-3 proteins have given rise to an increasing interest in this protein family as a novel target class for pharmacological intervention.[5,14,15,24–28] Since 14-3-3 proteins display no enzymatic activity and harbour no active site, a direct pharmacological approach has to include PPI modulation. Very recently, this possibility became a realistic option when the first small molecule 14-3-3 PPI inhibitors were reported by the groups of Yao, Botta, and Fu.[26–28] Complementary to inhibition, also the small-molecule stabilisation of PPIs is a feasible approach. Hence, adding to these successes, we have identified small molecules that are able to specifically stabilise a 14-3-3 protein–protein interaction.[22] In this attempt to find small molecules stabilising the PMA2–14-3-3 interaction, we have shown that the activity of a complex natural product (FC-A) can in part be substituted by synthetically much more accessible molecules.

Here we show how an initial primary screen hit (**1**) could be used as the starting point to establish a feasible structure-activity relationship (SAR) for stabilisation of a 14-3-3 protein–protein interaction. Crystallographic studies showed that replacement of the pyrrolinone backbone by a pyrazole orients one of the phenyl substituents closer into the rim of the 14-3-3–PMA2 interface; this is a promising binding site not addressed by **1** (Figure 3 f).

Although the potency of these molecules definitely needs further improvement, their structure provides proof-of-concept for the possibility of developing a rationale for the optimisation of small-molecule stabilisers of 14-3-3 PPIs. Apart from the complex natural products FC-A[18–23] and cotylenin A[30,31] and the recently published epibestatin and pyrrolidone1[22] small molecule stabilisers of 14-3-3 PPIs have not been identified.

In general, rational design and optimisation of small molecules with a PPI stabilising mode of action is in its infancy. Exceptions are the immunosuppressants FK506[32] and rapamycin[33] with their derivatives (AP1903, rapalogues)[34,35] and other chemically induced dimerisers frequently used in chemical biology basic research.[36,37] A strategy to success-

fully and specifically stabilise 14-3-3 PPIs would considerably expand the options available for active ingredient development in agriculture and the treatment of human disease, for example, in oncology, neurodegenerative diseases, cardiovascular diseases, obesity and diabetes.

Experimental Section

Chemical synthesis: All pyrrolinones were prepared by using a one-pot Doebner condensation[38] of a methylene component and a Schiff base. Pyrazoles were obtained by the treatment of the corresponding pyrrolinones with hydrazine (Scheme 1). The general procedure for the preparation of the methylene component is as follows. The acetophenone derivative (1.00 equiv) followed by diethyl oxalate (1.00 equiv) were added to a solution of sodium ethoxide (1.00 M, 1.10 equiv) in EtOH at 0 °C. The resulting suspension was stirred, overnight, at room temperature. Pentane was added and the mixture was filtered. The residue was washed with pentane and purified by recrystallisation.

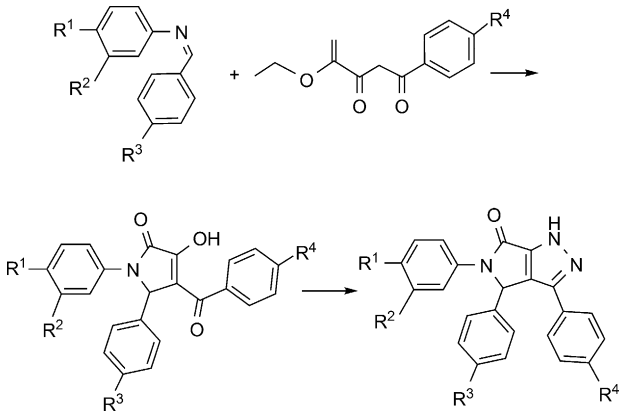

Scheme 1. Doebner condensation for the preparation of pyrrolinones and the formation of pyrazoles.

General procedure for the preparation of pyrrolinones (Table 1): The benzaldehyde derivative (1.00 equiv) followed by the aniline derivative (1.00 equiv) were added to a suspension (~0.06 M) of the methylene component (1.00 equiv) in acetic acid. The reaction mixture was stirred, overnight, at 90 °C. After being cooled to room temperature the mixture was diluted with Et_2O and filtered. The residue was washed with Et_2O to give the desired pyrrolinone derivative after drying (method A). Alternatively, the filtrate was evaporated and the residue was taken up in 1,4-dioxane and stirred for 45 min at 120 °C. After being cooled to room temperature the resulting suspension was filtered. The residue was washed with dioxane and dried, in vacuo, to give the desired pyrrolinone derivative (method B). The purity of the products was confirmed by RP-HPLC: C18 column (3 μm, CC 125/4), 0.5 mL min^{-1}, starting from ACN/water + 0.1% TFA 20:80 (2 min) to 100:0 in 40 min.

General procedure for the preparation of pyrazoles (Table 2): Hydrazine monohydrate (6.00 equiv) was added to a solution (0.06 M) of the corresponding pyrrolinone (1.00 equiv) in acetic acid. The reaction mixture was stirred for 2 h at 85 °C. After being cooled to room temperature water was added and the mixture was extracted three times with EtOAC. The combined organic layers were washed with brine, dried over $MgSO_4$ and the solvent was evaporated, in vacuo, to give the desired product.

Protein preparation: The tobacco 14-3-3e isoform deleted from its C-terminal 18 residues (T14-3eDC, amino acids 1–242 with a N-terminal RGS-$[His]_6$-tag, eGFP or GST-tag) was expressed in *E. coli* and purified as described before.[23] The C-terminal regions of PMA2 encompassing 30 or 66 amino acids (CT30, amino acids 927–956; CT66, amino acids 890–956) and characterised by the C-terminal tripeptide YDI were expressed as intein fusion peptides (IMPACT-CN, NEB) or GST fusions and purified as described before.[22,23]

Surface-based assay: A solution of GST–PMA2-CT66YDI (0.02 μg μL^{-1}) in Tris/HCl (25 mM, pH 7.5), $MgCl_2$ (2 mM) and NaCl (150 mM) was immobilised for 1 h at room temperature in a Costar 3925 96-well plate in a volume of 200 μL per well. Wells were blocked with Tris/HCl (25 mM, pH 7.5, 200 μL), $MgCl_2$ (2 mM), NaCl (150 mM), Tween-20 (0.05%) and BSA (1% w/v) for 1 h at room temperature followed by four washing steps at room temperature with Tris/HCl (25 mM, pH 7.5, 200 μL), $MgCl_2$ (2 mM), NaCl (150 mM) and Tween-20 (0.05%). Subsequently, wells were incubated for 2 h at 4 °C with Tris/HCl (25 mM, pH 7.5, 200 μL), $MgCl_2$ (2 mM), NaCl (150 mM) and Tween-20 (0.05%) BSA (0.1% w/v) containing T14-3c–EGFP (0.02 μg μL^{-1}) and test compound (100 μM). Four washing steps were performed as described above and EGFP fluorescence was measured by using the Infinite®F500 plate reader from Tecan.

Protein crystallography: T14-3e and PMA2-CT30 were mixed in a 1:1.4 ratio in HEPES (20 mM)/NaOH (pH 7.5), $MgCl_2$ (2 mM), DTT (2 mM) at a final concentration of 10 mg mL^{-1} and incubated, overnight, in the presence of the stabilising molecule **34**. Protein crystals were grown in hanging drops at 4 °C in CHES (0.1 M, pH 9.0), Na-citrate (1.0 M) and sucrose (30% w/v) by mixing equal volumes of protein complex and reservoir solution. After 2 days crystals appeared and grew within one week to dimensions of 300 × 200 × 200 μm. Crystals were directly transferred into liquid nitrogen for flash-cooling.

Data collection, structure determination and refinement: Data collection was performed in-house by using a Cu rotating anode (Rigaku) and was processed with XDS.[39] The previously solved structure with **1** (PDB ID: 3M51) was used for a first round of refinement. The obtained model was subjected to iterative rounds of model building and refinement by using the programs COOT and REFMAC.[40,41] Figures were prepared with PyMOL (www.pymol.org).

Acknowledgements

C.O. thanks BayerCrop Science, Bayer Healthcare, MerckSerono, and MSD for support.

[1] J. A. Wells, C. L. McClendon, *Nature* **2007**, *450*, 1001–1009.
[2] D. Bridges, G. B. Moorhead, *Sci STKE* **2005**, *296*, re10.
[3] C. Johnson, S. Crowther, M. J. Stafford, D. G. Campbell, R. Toth, C. MacKintosh, *Biochem. J.* **2010**, *427*, 69–78.
[4] M. B. Yaffe, K. Rittinger, S. Volinia, P. R. Caron, A. Aitken, H. Leffers, S. J. Gamblin, S. J. Smerdon, L. C. Cantley, *Cell* **1997**, *91*, 961–971.
[5] D. K. Morrison, *Trends Cell Biol.* **2009**, *19*, 16–23.
[6] W. J. Fantl, A. J. Muslin, A. Kikuchi, J. A. Martin, A. M. MacNicol, R. Gross, L. T. Williams, *Nature* **1994**, *371*, 612–614.
[7] M. Molzan, B. Schumacher, C. Ottmann, A. Baljuls, L. Polzien, M. Weyand, P. Thiel, R. Rose, M. Rose, P. Kuhenne, M. Kaiser, U. R. Rapp, J. Kuhlmann, C. Ottmann, *Mol. Cell. Biol.* **2010**, *30*, 4698–4711.
[8] D. S. Conklin, K. Galaktinov, D. Beach, *Proc. Natl. Acad. Sci. USA* **1995**, *92*, 7892–7896.
[9] C. Y. Peng, P. R. Graves, R. S. Thoma, Z. Wu, A. Shaw, *Science* **1997**, *277*, 1501–1505.
[10] A. Vassilev, K. J. Kaneko, H. Shu, Y. Zhao, M. L. DePamphilis, *Genes Dev.* **2001**, *15*, 1229–1241.
[11] B. Schumacher, M. Skwarczynska, R. Rose, C. Ottmann, *Acta Crystallogr. Sect. F Struct. Biol. Cryst. Commun.* **2010**, *66*, 978–984.
[12] S. Rajagopalan, R. S. Sade, F. M. Townsley, A. R. Fersht, *Nucleic Acids Res.* **2010**, *38*, 893–906.

[13] B. Schumacher, J. Mondry, P. Thiel, M. Weyand, C. Ottmann, *FEBS Lett.* **2010**, *584*, 1443–1448.
[14] H. Hermeking, *Nat. Rev. Cancer* **2003**, *3*, 931–943.
[15] D. Berg, C. Holzmann, O. Riess, *Nat. Rev. Neurosci.* **2003**, *4*, 752–762.
[16] H. Fu, J. Coburn, R. J. Collier, *Proc. Natl. Acad. Sci. USA* **1993**, *90*, 2320–2324.
[17] C. Ottmann, L. Yasmin, M. Weyand, J. L. Veesenmeyer, C. Diaz, R. H. Palmer, M. S. Francis, A. R. Hauser, A. Wittinghofer, B. Hallberg, *EMBO J.* **2007**, *26*, 902–913.
[18] A. Ballio, E. B. Chain, P. De Leo, B. F. Erlanger, M. Mauri, A. Tonolo, *Nature* **1964**, *203*, 297.
[19] C. Oecking, C. Eckerskorn, E. W. Weiler, *FEBS Lett.* **1994**, *352*, 163–166.
[20] M. Würtele, C. Jelich-Ottmann, A. Wittinghofer, C. Oecking, *EMBO J.* **2003**, *22*, 987–992.
[21] C. Oecking, M. Piotrowski, J. Hagemeier, K. Hagemann, *Plant J.* **1997**, *12*, 441–453.
[22] R. Rose, S. Erdmann, S. Bovens, A. Wolf, M. Rose, S. Hennig, H. Waldmann, C. Ottmann, *Angew. Chem.* **2010**, *122*, 4223–4226; *Angew. Chem. Int. Ed.* **2010**, *49*, 4129–4132.
[23] C. Ottmann, S. Marco, N. Jaspert, C. Marcon, N. Schauer, M. Weyand, C. Vandermeeren, G. Duby, M. Boutry, A. Wittinghofer, J. L. Rigaud, C. Oecking, *Mol. Cell* **2007**, *25*, 427–440.
[24] G. Tzivion, V. S. Gupta, L. Kaplun, V. Balan, *Semin. Cancer Biol.* **2006**, *16*, 203–213.
[25] R. K. Andrews, X. Du, M. C. Berndt, *Drug News Perspect.* **2007**, *20*, 285–292.
[26] H. Wu, J. Ge, S. Q. Yao, *Angew. Chem.* **2010**, *122*, 6678–6682; *Angew. Chem. Int. Ed.* **2010**, *49*, 6528–6532.
[27] V. Corradi, M. Mancini, F. Manetti, S. Petta, M. A. Santucci, M. Botta, *Bioorg. Med. Chem. Lett.* **2010**, *20*, 6133–6137.
[28] J. Zhao, Y. Du, J. R. Horton, A. K. Upadhyay, B. Lou, Y. Bai, X. Zhang, L. Du, M. Li, B. Wang, L. Zhang, J. T. Barbieri, F. R. Khuri, X. Cheng, H. Fu, *Proc. Natl. Acad. Sci. USA* **2011**, *108*, 16212–16216.
[29] P. Thiel, M. Kaiser, C. Ottmann, *Angew. Chem.* **2012**, *124*, 2052–2059.
[30] T. Sassa, T. Tojyo, K. Munakata, *Nature* **1970**, *227*, 379.
[31] C. Ottmann, M. Weyand, T. Sassa, T. Inoue, N. Kato, A. Wittinghofer, C. Oecking, *J. Mol. Biol.* **2009**, *386*, 913–919.
[32] J. Liu, J. D. Farmer, W. S. Lane, J. Friedman, I. Weissman, S. L. Schreiber, *Cell* **1991**, *66*, 807–815.
[33] E. J. Brown, M. W. Albers, T. B. Shin, K. Ichikawa, C. T. Keith, W. S. Lane, S. L. Schreiber, *Nature* **1994**, *369*, 756–758.
[34] T. Clackson, W. Yang, L. W. Rozamus, M. Hatada, J. F. Amara, C. T. Rollins, L. F. Stevenson, S. R. Magari, S. A. Wood, N. L. Courage, X. Lu, F. Cerasoli, M. Gilman, D. A. Holt, *Proc. Natl. Acad. Sci. USA* **1998**, *95*, 10437–10442.
[35] J. H. Bayle, J. S. Grimley, K. Stankunas, J. E. Gestwicki, T. J. Wandless, G. R. Crabtree, *Chem. Biol.* **2006**, *13*, 99–107.
[36] M. A. Farrar, J. Alberol-Ila, R. M. Perlmutter, *Nature* **1996**, *383*, 178–181.
[37] S. J. Kopytek, R. F. Standaert, J. C. Dyer, J. C. Hu, *Chem. Biol.* **2000**, *7*, 313–321.
[38] T. M. Kamenecka, S. J. Danishefsky, *Chem. Eur. J.* **2001**, *7*, 41–63; b) A. Martín, M. Atlabe, S. Filippone, A. Martín Domenech, L. Echegoyen, C. M. Cardona, *Angew. Chem.* **2006**, *118*, 116–120; *Angew. Chem. Int. Ed.* **2006**, *45*, 7430–7433.
[39] W. Kabsch, *J. Appl. Crystallogr.* **1993**, *26*, 795–800.
[40] P. Emsley, K. Cowtan, *Acta. Cryst. D* **2004**, *60*, 2126–2132.
[41] G. N. Murshudov, A. A. Vagin, E. J. Dodson, *Acta. Cryst. D* **1997**, *53*, 240–255.

Received: November 30, 2011
Published online: ■■ ■■, 2012

Glued together: An initial screening hit that stabilises a 14-3-3 protein–protein interaction has been optimised by means of chemical synthesis. The resulting compound is three-times more active than the initial hit and displays selectivity for the interaction of 14-3-3 proteins with the plant proton pump PMA2 (see figure).

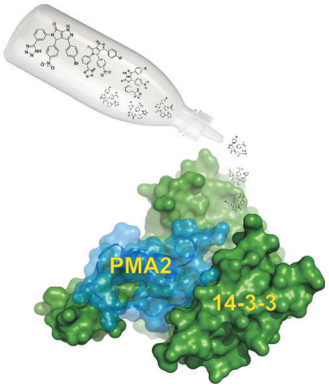

Protein–Protein Interactions

A. Richter, R. Rose, C. Hedberg, H. Waldmann, C. Ottmann** ..... ▮▮▮▮–▮▮▮▮

An Optimised Small-Molecule Stabiliser of the 14-3-3–PMA2 Protein–Protein Interaction